Noncollective excitations in low-energy heavy-ion reactions: Applicability of the random-matrix model

S. Yusa,[1] K. Hagino,[1] and N. Rowley[2]
[1]*Department of Physics, Tohoku University, Sendai 980-8578, Japan*
[2]*Institut de Physique Nucléaire, UMR 8608, CNRS-IN2P3 et Université de Paris Sud, 91406 Orsay Cedex, France*
(Received 29 August 2013; published 30 October 2013)

We investigate the applicability of a random-matrix model to the description of noncollective excitations in heavy-ion reactions around the Coulomb barrier. To this end, we study fusion in the reaction ^{16}O + ^{208}Pb, taking account of the known noncollective excitations in the ^{208}Pb nucleus. We show that the random-matrix model for the corresponding couplings reproduces reasonably well the exact calculations, obtained using empirical deformation parameters. This implies that the model may provide a powerful method for systems in which the noncollective couplings are not so well known.

DOI: 10.1103/PhysRevC.88.044620 PACS number(s): 24.10.Eq, 24.60.−k, 25.70.Jj

I. INTRODUCTION

Heavy-ion reactions around the Coulomb barrier often show a behavior that cannot be accounted for by a simple potential model [1–3]. They have thus provided a good opportunity to investigate the role of internal degrees of freedom in the reaction process. One of the well known examples is a large enhancement of sub-barrier fusion cross sections due to the couplings between the relative motion of the projectile and target nuclei and their internal degrees of freedom, such as surface vibrations for spherical nuclei, or rotational motion for nuclei possessing a static, intrinsic deformation. It is well recognized that these couplings lead to a distribution of potential barriers [4], and a method was proposed by Rowley, Satchler, and Stelson to extract the barrier distributions directly from experimental fusion cross sections [5]. The barrier distributions extracted in this way are found to be sensitive to details of the couplings, often showing a characteristic structured behavior [1,6,7]. Similar heavy-ion barrier distributions can also be defined for large-angle quasielastic scattering [8,9].

In order to analyze experimental data for these low-energy heavy-ion reactions, the coupled-channels method has been employed as a standard approach [3,10]. This method describes the reaction in terms of the internal excitations of the colliding nuclei, representing the total wave function of the system as a superposition of wave functions for the relevant reaction channels. Conventionally, a few low-lying collective excitations, that are strongly coupled to the ground state, are taken into account in these calculations. Such analyses have successfully accounted for the strong enhancement of sub-barrier fusion cross sections, and have successfully reproduced the structure of the fusion and quasielastic barrier distributions for many systems [1,3].

Recently, quasielastic barrier distributions have been measured for the ^{20}Ne + ^{90,92}Zr systems [11]. The corresponding coupled-channels calculations show that the main structure of these barrier distributions is determined by the rotational excitations of the strongly deformed nucleus ^{20}Ne. The calculated barrier distributions are in fact almost identical for the two systems, even when the collective excitations of the Zr isotopes are taken into account. It was, therefore, surprising when the two experimental barrier distributions were found to be different in an important respect. That is, the barrier distribution for ^{20}Ne + ^{92}Zr exhibits a much more smeared behavior than that for the ^{20}Ne + ^{92}Zr system. The origin of this difference has been conjectured in Ref. [11] to be the multitude of noncollective excitations of the Zr isotopes, that are generally ignored in a coupled-channels analysis. In fact, the two extra neutrons in the ^{92}Zr nucleus lead to a significantly larger number of non-collective excited states compared with ^{90}Zr, since this latter possesses an $N = 50$ closed shell (the difference is reflected by the number of known states up to an excitation energy of 5 MeV; one finds 35 for ^{90}Zr and 87 for ^{92}Zr [12]).

There are many ways to describe noncollective excitations in heavy-ion reactions [13–24]. In the 1970s, Weidenmüller *et al*. introduced a random-matrix model for such excitations in order to study deep inelastic collisions [18–24]. See also Ref. [25], in which a link between the coupled-channels approach and the random-matrix model has been made. In Ref. [13], we have used a similar model in a schematic one-dimensional barrier-penetration problem, in order to study the role of these noncollective excitations in low-energy reactions. On the other hand, in Ref. [14], we have explicitly taken into account in the coupled-channels formalism all of the 70 known noncollective states in ^{208}Pb below 7.382 MeV [26,27] without resorting to the random-matrix model, and have analysed in this way the experimental data for the ^{16}O + ^{208}Pb reaction. Although some discrepancies between the experimental and theoretical barrier distributions remain after the inclusion of noncollective excitations, we have shown in Ref. [14] that these excitations play a more important role as the incident energy increases. We have also compared there the role of noncollective excitations in the fusion and quasielastic barrier distributions, and have shown that they affect both distributions in a similar fashion.

Given that exact calculations with a realistic spectrum for noncollective states is possible here, it is intriguing to also apply the random-matrix model to this system in order to test its applicability. This theoretical test is the main aim of this paper, and we achieve it by comparing our new results with those obtained in Ref. [14]. Note that, in contrast to ^{208}Pb, the properties of the noncollective states in ^{90,92}Zr are not known

sufficiently well. As we will show in this paper, the random-matrix model provides a good method for a description of noncollective excitations in such a situation.

The paper is organized as follows. In Sec. II, we explain the coupled-channels formalism with noncollective excitations based on the random-matrix model. In Sec. III, we discuss the strength distribution and fusion cross sections obtained with this model. We then compare these with calculations using the more exact couplings and discuss the applicability of the random-matrix model. The paper is summarized in Sec. IV.

II. COUPLED-CHANNELS METHOD WITH NONCOLLECTIVE EXCITATIONS

In order to describe internal excitations during the reaction process, we assume the following Hamiltonian:

$$H = -\frac{\hbar^2}{2\mu}\nabla^2 + V_{\rm rel}(r) + H_0(\{\xi\}) + V_{\rm coup}(\boldsymbol{r}, \{\xi\}), \quad (1)$$

where $\boldsymbol{r}$ is the separation of the projectile and target nuclei, and μ is the reduced mass. In this equation, $H_0(\{\xi\})$ is the intrinsic Hamiltonian with $\{\xi\}$ representing a set of internal degrees of freedom. The optical potential for the relative motion is $V_{\rm rel}(r)$, and it includes an imaginary part to simulate the fusion process (that is, strong absorption into compound-nucleus degrees of freedom inside the Coulomb barrier). The coupling Hamiltonian between the relative motion and the intrinsic degrees of freedom is denoted by $V_{\rm coup}(\boldsymbol{r}, \{\xi\})$.

The coupled-channels equations for this Hamiltonian are obtained by expanding the total wave function in terms of the eigenfunctions of $H_0(\{\xi\})$. The equations read

$$\left[-\frac{\hbar^2}{2\mu}\frac{d^2}{dr^2} + \frac{J(J+1)\hbar^2}{2\mu r^2} + V_{\rm rel}(r) + \epsilon_n - E\right]u_n^J(r) + \sum_m V_{nm}(r)u_m^J(r) = 0, \quad (2)$$

where ϵ_n is the excitation energy for the nth channel. In deriving these equations, we have employed the iso-centrifugal approximation [3,28–33]. In this approximation, the orbital angular momentum in the centrifugal potential is replaced by the total angular momentum J, thereby considerably reducing the dimension of the coupled-channels equations.

In solving these equations, we impose the following asymptotic boundary conditions

$$u_n^J(r) \to H_J^{(-)}(k_n r)\delta_{n,0} - \sqrt{\frac{k_0}{k_n}}S_n^J H_J^{(+)}(k_n r), \quad (3)$$

for $r \to \infty$, together with the regular boundary condition at the origin. Here, $k_n = \sqrt{2\mu(E-\epsilon_n)/\hbar^2}$ is the wave number for the nth channel, where $n = 0$ corresponds to the entrance channel. S_n^J is the nuclear S matrix, and $H_J^{(-)}(kr)$ and $H_J^{(+)}(kr)$ are the incoming and the outgoing Coulomb wave functions, respectively. The fusion cross sections are then obtained as

$$\sigma_{\rm fus}(E) = \frac{\pi}{k_0^2}\sum_J (2J+1)\left(1 - \sum_n \left|S_n^J\right|^2\right). \quad (4)$$

In the random-matrix model [18–25], one assumes an ensemble of coupling matrix elements whose first moment satisfies

$$\overline{V_{nn'}^{II'}(r)} = 0, \quad (5)$$

while the second moment satisfies

$$\overline{V_{nn'}^{II'}(r)V_{n''n'''}^{I''I'''}(r')} = \{\delta_{nn''}\delta_{n'n'''}\delta_{II''}\delta_{I'I'''} + \delta_{nn'''}\delta_{n'n''}\delta_{II'''}\delta_{I'I''}\} \times \sqrt{(2I+1)(2I'+1)}\sum_\lambda \begin{pmatrix} I & \lambda & I' \\ 0 & 0 & 0 \end{pmatrix}^2 \times \alpha_\lambda(n, n'; I, I'; r, r'). \quad (6)$$

Here, I is the spin of the intrinsic state labeled by n, and α_λ is the coupling form factor. Weidenmüller *et al.* analytically carried out the ensemble average by assuming a weak coupling limit [18–25]. In contrast, we take the ensemble average numerically in our calculations in order to avoid the approximations (but see Sec. III B below). Notice that the transport equation derived in the random matrix model has to be solved numerically in any case, even if the ensemble average of the coupling matrix elements can be performed analytically.

In this paper, for simplicity, we assume that the noncollective excitations couple only to the ground state, as in the linear coupling approximation employed in our previous work [14]. For the form factor α_λ, we assume the following dependence:

$$\alpha_\lambda(n, 0; I, 0; r, r') = \frac{w_\lambda}{\sqrt{\rho(\epsilon_n)}}e^{-\frac{\epsilon_n^2}{2\Delta^2}}e^{-\frac{(r-r')^2}{2\sigma^2}}h(r)h(r'), \quad (7)$$

where $\rho(\epsilon_n)$ is the level density at an excitation energy ϵ_n, and $(w_\lambda, \Delta, \sigma)$ are adjustable parameters. The appearance of the level density in the denominator reflects the complexity of the noncollective excited states, as discussed in Ref. [21]. For the function $h(r)$, we adopt the derivative of the Woods-Saxon potential, that is,

$$h(r) = \frac{e^{(r-R)/a}}{[1+e^{(r-R)/a}]^2}. \quad (8)$$

Note that this choice of the form factor corresponds to the coupling Hamiltonian in the linear coupling approximation derived from the Woods-Saxon potential.

III. APPLICABILITY OF THE RANDOM-MATRIX MODEL

A. Strength distribution

Let us now apply the random-matrix model to the ^{16}O + ^{208}Pb reaction and discuss its applicability. As we mentioned in Sec. I, we have studied this system by explicitly including 70 noncollective states below 7.382 MeV, together with a few collective states, in the coupled-channels calculations [14]. The effect of the noncollective couplings was found to be non-negligible and tends to result in a widening of the barrier distribution. In this paper, we attempt to model the couplings to these 70 noncollective states with the random-matrix model. The aim here is to show that the random-matrix model is a good alternative to the exact calculation, and could

be important in cases where the experimental information on the noncollective states is not fully available.

We first discuss the strength distribution for the noncollective excitations in ^{208}Pb obtained with the random-matrix model. To this end, we define the strength distribution as

$$b_I = \sqrt{\sum_\lambda \begin{pmatrix} 0 & \lambda & I \\ 0 & 0 & 0 \end{pmatrix}^2 \sqrt{\frac{2I+1}{\rho(\epsilon)}} e^{-\frac{\epsilon^2}{2\Delta^2}}} = \sqrt{\sqrt{\frac{2I+1}{\rho(\epsilon)}} e^{-\frac{\epsilon^2}{2\Delta^2}}}. \tag{9}$$

This quantity essentially corresponds to the square root of Eq. (6), except for an overall scale factor (here we have assumed $w_\lambda = w$ for all λ and omitted w_λ in the definition for the strength function).

The level density in Eq. (9) is treated in the following way. It is originally defined by

$$\rho(\epsilon) = \sum_n \delta(\epsilon - \epsilon_n) \tag{10}$$

for a discrete spectrum. For practical purposes, we define the function

$$N(\epsilon) = \int_0^\epsilon \rho(\epsilon')d\epsilon' = \sum_n \theta(\epsilon - \epsilon_n), \tag{11}$$

that gives the number of levels up to the excitation energy ϵ. We fit this function with a polynomial in ϵ, and then define a continuous level density by differentiating this polynomial. Figure 1 shows the experimental $N(\epsilon)$ for ^{208}Pb [26] in the interval between 4 and 7.5 MeV (solid line) and its fit with a polynomial $f(\epsilon) = \sum_{n=0}^{6} a_n \epsilon^n$ (dashed line). The values of a_n are $a_0 = -7479$, $a_1 = 6969$ (MeV^{-1}), $a_2 = -2612$ (MeV^{-2}), $a_3 = 497.5$ (MeV^{-3}), $a_4 = -49.59$ (MeV^{-4}), $a_5 = 2.347$ (MeV^{-5}), and $a_6 = -0.03632$ (MeV^{-6}). The continuous level density, $\rho(\epsilon) = df(\epsilon)/d\epsilon$, is shown in Fig. 2.

The strength distribution b_I calculated with this level density is shown in Fig. 3 by the solid line as a function of excitation energy ϵ. The parameter Δ in Eq. (9) is chosen to be 7 MeV, as in Refs. [23,24]. For comparison, the figure also shows the distribution of the experimental deformation parameters β_I [26], smeared with a Gaussian function with a width of 0.15 MeV (dashed line). We have also performed the same smearing for the strength distribution b_I. Also, since the dimensions of β_I and b_I are not the same, the deformation parameters β_I are scaled by a factor 10 so that the heights of the first peaks at about 4.3 MeV match one another. Although there exists a small deviation for the peaks between 5 and 7 MeV, the overall structure of the strength distribution is well reproduced by this model.

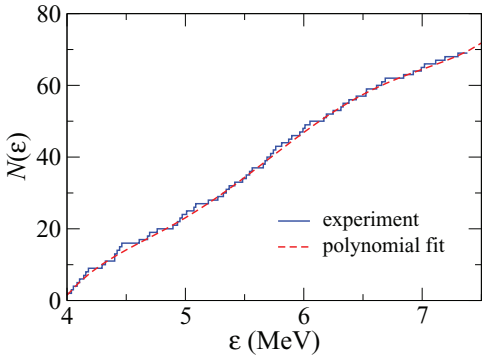

FIG. 1. (Color online) The number of levels of the ^{208}Pb nucleus up to the excitation energy ϵ as a function of ϵ. The histogram represents the experimental data [26], while the dashed line shows its fit with a polynomial function up to the sixth order.

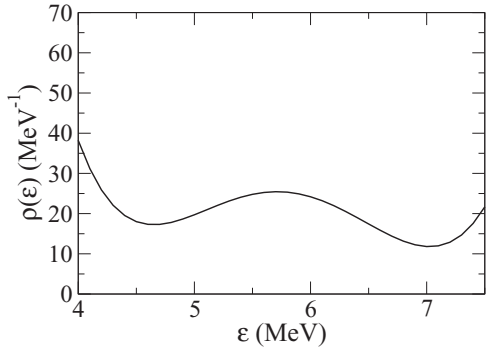

FIG. 2. The continuous level density for ^{208}Pb obtained as a first derivative of the fitting function $f(\epsilon)$ shown in Fig. 1.

B. Fusion cross sections

The strength distribution discussed in the previous subsection determines the coupling strength to each excited state. Let us then examine how the random-matrix model can be compared with the exact results in terms of the fusion cross sections for the ^{16}O + ^{208}Pb system. For this purpose, we use the same Woods-Saxon potential for the nuclear potential as in Ref. [14]; it has a surface diffuseness $a = 0.671$ fm, a radius $R = 8.39$ fm, and a depth $V_0 = 550$ MeV. For the couplings to the collective excitations, we take into account the vibrational 3^- state at 2.615 MeV, the 5^- state at 3.198 MeV, and the 2^+ state at 4.085 MeV in ^{208}Pb. The octupole mode is included up to the two-phonon states, while the other, weaker, vibrational modes are taken into account only up

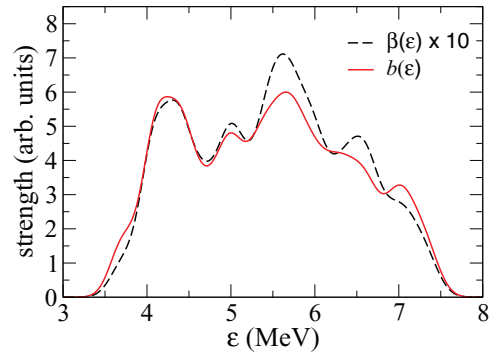

FIG. 3. (Color online) The strength distributions for ^{208}Pb as a function of excitation energy ϵ. The dashed line shows the distribution of the experimental deformation parameters, while the solid line is obtained based on the random-matrix model using Eq. (9). Both distributions are smeared with a Gaussian function with a width of 0.15 MeV. An overall scaling factor is introduced to the dashed line as the dimension is different between the two curves (see text).

to their one-phonon states. The deformation parameters for these vibrational modes are estimated from the measured electromagnetic transition probabilities. They are $\beta_3 = 0.122$, $\beta_5 = 0.058$, and $\beta_2 = 0.058$ together with a radius parameter of $r_0 = 1.2$ fm. Although we took into account the octupole phonon state of ^{16}O in our preivous study [14], for simplicity we do not include it in the present calculations, since its effect can be well described by an adiabatic renormalization of the potential depth [3,34]. For the parameter σ in Eq. (7), we follow Refs. [23,24] and use $\sigma = 4$ fm. On the other hand, the parameter $w_\lambda = w$ is chosen to be $w = 38\,000$ MeV$^{3/2}$ so that the height of the main peak in the fusion barrier distribution is reproduced by the random-matrix model. In principle one should repeat the coupled-channels calculations many times with randomly generated matrix elements and take an ensemble average. However, we have found in a smaller model space that the dispersion due to the randomness of these elements is sufficiently small that a single realization already yields reasonable results. We therefore take only a single set of the coupling matrix in the calculations shown below, without taking an ensemble average of the results.

Figures 4(a) and 4(b) show the ^{16}O + ^{208}Pb fusion excitation function on linear and logarithmic scales respectively. The dashed lines show the results obtained with the *measured* deformation parameters for the noncollective excitations, while the solid lines show the results obtained using the random-matrix approximation. For comparison, the dotted lines show results that account only for the collective excitations. Although a small overall shift can be seen, it is clear that the random-matrix model reproduces the exact results reasonably well.

In order to highlight the energy dependence, Fig. 4(c) shows the fusion barrier distribution $D_{\rm fus}(E) = d^2(E\sigma_{\rm fus})/dE^2$ [1,3,5,6]. Although the main peak is slightly shifted in energy, this confirms that the random-matrix model reproduces well the exact results. That is, with respect to the dotted line, the change in the energy dependence of fusion cross sections due to the noncollective excitations is similar in the two calculations. In particular, both barrier distributions are smeared out in a similar way at energies around 80 MeV, and both calculations yield a similar second peak around 87.5 MeV. (We note that if the strength w_0 was somewhat larger, the second peak could appear at even higher energies, possibly reflecting the broad bump seen at around 97 MeV in the experimental data.)

As we have argued in Ref. [13], the higher-energy peaks in the barrier distribution are affected more by noncollective excitations than are the lower-energy peaks. Unfortunately this is not easy to see in Fig. 4 because the peaks obtained with purely collective couplings are not resolved. This difference can, however, be easily understood using perturbation theory. That is, the eigenchannels corresponding to the higher-energy peaks in the barrier distribution couple more strongly to the noncollective states via their ground-state component simply because the energy differences are smaller. Higher peaks are thus redistributed more, effectively removing much of their strength from that region of energy.

From these calculations, it is evident that the effects of noncollective excitations are not sensitive to details of the noncollective couplings, and that the random-matrix model is applicable to the description of noncollective excitations, so long as the relevant parameters are chosen appropriately.

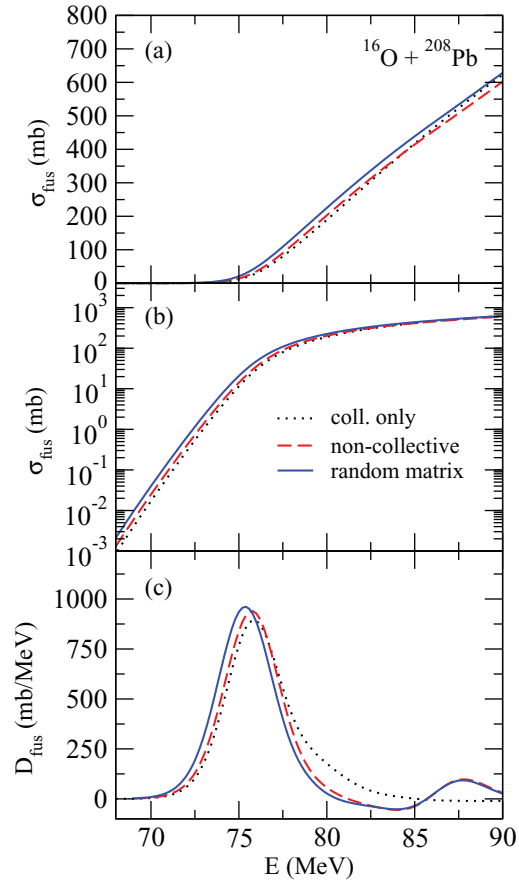

FIG. 4. (Color online) (a), (b) Fusion cross sections $\sigma_{\rm fus}$ and (c) fusion barrier distributions $D_{\rm fus}(E) = d^2E\sigma_{\rm fus}(E)dE^2$ for the ^{16}O + ^{208}Pb system obtained from three different calculations. Dashed lines show results obtained with the experimental, noncollective deformation parameters, whereas the solid lines are obtained from the random-matrix model. Dotted lines result from calculations that include only the ^{208}Pb collective excitations.

IV. SUMMARY

We have investigated the applicability of the random-matrix model for the description of noncollective excitations in low-energy heavy-ion reactions. To this end, we have calculated the fusion excitation function for the ^{16}O + ^{208}Pb system, where the role of the noncollective excitations has already been investigated in our previous study using empirical deformation parameters.

We have first shown that the coupling strength distribution obtained with the random-matrix model agrees well with the experimental distribution. The fusion cross section and barrier distribution for the ^{16}O + ^{208}Pb system obtained with empirical noncollective couplings are also well reproduced by the random-matrix model with appropriately chosen parameters. These results provide a validation of the random-matrix model for the description of noncollective couplings.

For the ^{208}Pb nucleus, detailed properties of noncollective states are known over a large energy range. However, this is not always the case for other systems. That is, for many nuclei, even though the energies and spin-parity may be relatively well known for many noncollective states, the coupling strengths are poorly determined. In such a situation, the present study suggests that the random matrix model provides a powerful tool to treat these coupling strengths. A good example is the quasielastic barrier distribution for the ^{20}Ne + ^{90,92}Zr systems, where it has been suggested that noncollective excitations may play an important role. Analyses for these systems within the random-matrix model are under way. We shall report the results in a separate publication [35].

ACKNOWLEDGMENTS

This work was supported by the Global COE Program "Weaving Science Web beyond Particle-Matter Hierarchy" at Tohoku University, and by the Japanese Ministry of Education, Culture, Sports, Science and Technology by Grant-in-Aid for Scientific Research under Program No. (C) 22540262.

[1] M. Dasgupta, D. J. Hinde, N. Rowley, and A. M. Stefanini, Annu. Rev. Nucl. Part. Sci. **48**, 401 (1998).
[2] A. B. Balantekin and N. Takigawa, Rev. Mod. Phys. **70**, 77 (1998).
[3] K. Hagino and N. Takigawa, Prog. Theor. Phys. **128**, 1061 (2012).
[4] C. H. Dasso, S. Landowne, and A. Winther, Nucl. Phys. A **405**, 381 (1983); **407**, 221 (1983).
[5] N. Rowley, G. R. Satchler, and P. H. Stelson, Phys. Lett. B **254**, 25 (1991).
[6] J. R. Leigh *et al*., Phys. Rev. C **52**, 3151 (1995).
[7] J. R. Leigh, N. Rowley, R. C. Lemmon, D. J. Hinde, J. O. Newton, J. X. Wei, J. C. Mein, C. R. Morton, S. Kuyucak, and A. T. Kruppa, Phys. Rev. C **47**, R437 (1993).
[8] H. Timmers, J. R. Leigh, M. Dasgupta, D. J. Hinde, R. C. Lemmon, J. C. Mein, C. R. Morton, J. O. Newton, and N. Rowley, Nucl. Phys. A **584**, 190 (1995).
[9] K. Hagino and N. Rowley, Phys. Rev. C **69**, 054610 (2004).
[10] K. Hagino, N. Rowley, and A. T. Kruppa, Comput. Phys. Commun. **123**, 143 (1999).
[11] E. Piasecki, Ł. Świderski, W. Gawlikowicz, J. Jastrzebski, N. Keeley, M. Kisieliński, S. Kliczewski, A. Kordyasz, M. Kowalczyk, S. Khlebnikov, E. Koshchiy, E. Kozulin, T. Krogulski, T. Loktev, M. Mutterer, K. Piasecki, A. Piórkowska, K. Rusek, A. Staudt, M. Sillanpää, S. Smirnov, I. Strojek, G. Tiourin, W. H. Trzaska, A. Trzcińska, K. Hagino, and N. Rowley, Phys. Rev. C **80**, 054613 (2009).
[12] Brookhaven National Laboratory, Evaluated Nuclear Structure Data File, http://www.nndc.bnl.gov/ensdf/, and references therein.
[13] S. Yusa, K. Hagino, and N. Rowley, Phys. Rev. C **82**, 024606 (2010).
[14] S. Yusa, K. Hagino, and N. Rowley, Phys. Rev. C **85**, 054601 (2012).
[15] A. Diaz-Torres, D. J. Hinde, M. Dasgupta, G. J. Milburn, and J. A. Tostevin, Phys. Rev. C **78**, 064604 (2008).
[16] A. Diaz-Torres, Phys. Rev. C **81**, 041603(R) (2010).
[17] A. Diaz-Torres, Phys. Rev. C **82**, 054617 (2010).
[18] C. M. Ko, H. J. Pirner, and H. A. Weidenmüller, Phys. Lett. B **62**, 248 (1976).
[19] D. Agassi, H. A. Weidenmüller, and C. M. Ko, Phys. Lett. B **73**, 284 (1978).
[20] B. R. Barrett, S. Shlomo, and H. A. Weidenmüller, Phys. Rev. C **17**, 544 (1978).
[21] D. Agassi, C. M. Ko, and H. A. Weidenmüller, Ann. Phys. (N.Y.) **107**, 140 (1977).
[22] C. M. Ko, D. Agassi, and H. A. Weidenmüller, Ann. Phys. (N.Y.) **117**, 237 (1979).
[23] D. Agassi, C. M. Ko, and H. A. Weidenmüller, Ann. Phys. (N.Y.) **117**, 407 (1979).
[24] D. Agassi, C. M. Ko, and H. A. Weidenmüller, Phys. Rev. C **18**, 223 (1978).
[25] C. M. Ko, Z. Phys. A **286**, 405 (1978).
[26] W. T. Wagner, G. M. Crawley, G. R. Hammerstein, and H. McManus, Phys. Rev. C **12**, 757 (1975).
[27] M. B. Lewis, F. E. Bertrand, and C. B. Fulmer, Phys. Rev. C **7**, 1966 (1973).
[28] R. Lindsay and N. Rowley, J. Phys. G **10**, 805 (1984).
[29] M. A. Nagarajan, N. Rowley, and R. Lindsay, J. Phys. G **12**, 529 (1986).
[30] M. A. Nagarajan, A. B. Balantekin, and N. Takigawa, Phys. Rev. C **34**, 894 (1986).
[31] H. Esbensen, S. Landowne, and C. Price, Phys. Rev. C **36**, 1216 (1987); **36**, 2359 (1987).
[32] O. Tanimura, Phys. Rev. C **35**, 1600 (1987); Z. Phys. A **327**, 413 (1987).
[33] J. Gomez-Camacho, M. V. Andres, and M. A. Nagarajan, Nucl. Phys. A **580**, 156 (1994).
[34] N. Takigawa, K. Hagino, M. Abe, and A. B. Balantekin, Phys. Rev. C **49**, 2630 (1994).
[35] S. Yusa, K. Hagino, and N. Rowley, arXiv:1309.4674.